LUND UNIVERSITY

Effective Density and Mixing State of Aerosol Particles in a Near-Traffic Urban Environment.

Rissler, Jenny; Nordin, Erik; Eriksson, Axel; Nilsson, Patrik; Frosch, Mia; Sporre, Moa; Wierzbicka, Aneta; Svenningsson, Birgitta; Löndahl, Jakob; Messing, Maria; Sjögren, Staffan; Hemmingsen, Jette G; Loft, Steffen; Pagels, Joakim; Swietlicki, Erik

Published in:
Environmental Science & Technology

DOI:
10.1021/es5000353

2014

Link to publication

Citation for published version (APA):
Rissler, J., Nordin, E., Eriksson, A., Nilsson, P., Frosch, M., Sporre, M., Wierzbicka, A., Svenningsson, B., Löndahl, J., Messing, M., Sjögren, S., Hemmingsen, J. G., Loft, S., Pagels, J., & Swietlicki, E. (2014). Effective Density and Mixing State of Aerosol Particles in a Near-Traffic Urban Environment. *Environmental Science & Technology*, *48*(11), 6300-6308. https://doi.org/10.1021/es5000353

Total number of authors:
15

General rights
Unless other specific re-use rights are stated the following general rights apply:
Copyright and moral rights for the publications made accessible in the public portal are retained by the authors and/or other copyright owners and it is a condition of accessing publications that users recognise and abide by the legal requirements associated with these rights.
• Users may download and print one copy of any publication from the public portal for the purpose of private study or research.
• You may not further distribute the material or use it for any profit-making activity or commercial gain
• You may freely distribute the URL identifying the publication in the public portal

Read more about Creative commons licenses: https://creativecommons.org/licenses/

Take down policy
If you believe that this document breaches copyright please contact us providing details, and we will remove access to the work immediately and investigate your claim.

LUND UNIVERSITY

PO Box 117
221 00 Lund
+46 46-222 00 00

Download date: 26. Apr. 2024

Environmental Science & Technology

Article

pubs.acs.org/est

Terms of Use CC-BY

Effective Density and Mixing State of Aerosol Particles in a Near-Traffic Urban Environment

Jenny Rissler,*[,†] Erik Z. Nordin,[†] Axel C. Eriksson,[‡] Patrik T. Nilsson,[†] Mia Frosch,[‡,#] Moa K. Sporre,[‡] Aneta Wierzbicka,[†] Birgitta Svenningsson,[‡] Jakob Löndahl,[†] Maria E. Messing,[§] Staffan Sjogren,[‡,⊥] Jette G. Hemmingsen,[∥] Steffen Loft,[∥] Joakim H. Pagels,[†] and Erik Swietlicki[‡]

[†]Ergonomics and Aerosol Technology, [‡]Division of Nuclear Physics, and [§]Solid State Physics, Lund University, P.O. Box 118, SE-221 00, Lund, Sweden

[∥]Section of Environmental Health, Dept. of Public Health, University of Copenhagen, Postboks 209, 1014 København K, Denmark

Supporting Information

ABSTRACT: In urban environments, airborne particles are continuously emitted, followed by atmospheric aging. Also, particles emitted elsewhere, transported by winds, contribute to the urban aerosol. We studied the effective density (mass-mobility relationship) and mixing state with respect to the density of particles in central Copenhagen, in wintertime. The results are related to particle origin, morphology, and aging. Using a differential mobility analyzer-aerosol particle mass analyzer (DMA-APM), we determined that particles in the diameter range of 50−400 nm were of two groups: porous soot aggregates and more dense particles. Both groups were present at each size in varying proportions. Two types of temporal variability in the relative number fraction of the two groups were found: soot correlated with intense traffic in a diel pattern and dense particles increased during episodes with long-range transport from polluted continental areas. The effective density of each group was relatively stable over time, especially of the soot aggregates, which had effective densities similar to those observed in laboratory studies of fresh diesel exhaust emissions. When heated to 300 °C, the soot aggregate volatile mass fraction was ∼10%. For the dense particles, the volatile mass fraction varied from ∼80% to nearly 100%.

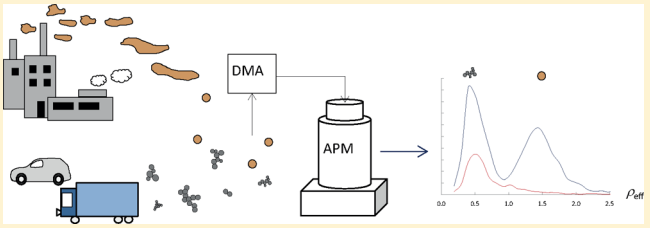

INTRODUCTION

Exposure to particulate matter (PM) is associated with adverse health effects ranging from acute cardiovascular and respiratory disease to increased mortality rates and cancer.[1,2] In urban environments, where both PM concentrations and population exposure are typically high, the aerosol consists of a complex mixture of particles from multiple local sources superimposed on a variable background of particles in air masses brought from near or far. Soot particles are ubiquitous in urban environments with diesel vehicles and residential wood combustion as major sources.[3] Recently, the World Health Organization's (WHO) affiliated International Agency for Research on Cancer (IARC) classified diesel engine exhaust—which is rich in soot—as carcinogenic to humans.[4,5] As summarized by WHO, new epidemiological and toxicological evidence also links black carbon, or soot particles, to cardiovascular health effects.[6] This suggests that soot concentrations provide an important additional parameter in the understanding of the health effects of particulate substances from combustion sources (especially traffic). Throughout this paper, we use the term "soot particle" for primary particle emissions from incomplete combustion of hydrocarbon-containing fuels at high temperatures and low oxygen conditions, dominated by elemental carbon. Soot particles are typically aggregates built up by 10−40 nm spherules of graphite-like structure, typically with an organic coating and traces of metals.[7,8]

Aerosol instruments based on the differential mobility analyzer (DMA) are widely used for the characterization of ambient submicrometer particle number size distributions. The DMA classifies particles according to their equivalent mobility diameter, d_m (closely related to the thermodynamic equivalent diameter), which also largely determines the deposition probability and deposition site in the respiratory tract, for spherical as well as nonspherical particles (if <400 nm with densities <2 g/cm^3).[9,10] The size and shape of inhaled particles also determine the particle surface area and its related reactivity and carrier functions, as well as the possible systemic translocation.[1]

Even though the mobility diameter of the particle determines the deposition in the respiratory tract, the estimation of dose to the lung with respect to surface area or mass requires additional information related to the particle structure, especially for soot aggregates, that is far from spherical. Current estimates of the

Received: January 7, 2014
Revised: May 2, 2014
Accepted: May 5, 2014
Published: May 5, 2014

 © 2014 American Chemical Society

dose deposited in the respiratory system are typically based on assumptions of spherical particles of unit density (e.g., Hussein et al.[11]). It is known that for porous particles, such as aggregates, this assumption may lead to overestimating the deposited dose with respect to particle mass, while underestimating surface area.[9,12] In a few studies, more complex assumptions about particle effective density[13−16] were used; however, ambient data on which to base such assumptions are largely lacking.

Numerous laboratory studies on the characteristics of fresh soot particles have examined the particle mass-mobility relationship and/or effective density.[9,17−22] Several of these studies have shown that the mass-mobility relationship of particles formed in diffusion-limited processes often can be described by a power law function:

$$m_{agg}(d_m) = K d_m^{\varepsilon_m} \quad (1)$$

where m_{agg} is the agglomerate mass, K is a constant, and ε_m is the mass-mobility exponent, typically, 2.3 ± 0.2 when determined experimentally. This is close to the exponent predicted by the theory of particles formed by diffusion-limited cluster aggregation of 2.2.[23] We define effective density as the mass divided by the volume of a sphere of the same d_m according to

$$\rho_{eff}(d_m) = \frac{6m}{\pi d_m^3} = \frac{6K \cdot d_m^{\varepsilon_m - 3}}{\pi} \quad (2)$$

As soon as the soot particles are emitted to the atmosphere, the atmospheric aging process is initiated involving photochemical aging, condensation, and coagulation.[24] Secondary material (typically hygroscopic) will condense onto the soot surface, and the agglomerate will eventually collapse through interaction with atmospheric water or other components with sufficiently high surface tension.[25,26] The atmospheric soot aging process and the time scales involved are still not understood to the extent that the health and climate impacts of the soot in an urban plume can be satisfactorily estimated in air quality models. The conversion from fresh and hydrophobic soot particles to aged and hygroscopic particles is often modeled as a first-order system with a single parameter representing the time scale on which a population of soot particles transfers from the "fresh" category to the "aged" category.[27]

The mass-mobility relationship or effective density can be measured using the DMA-aerosol particle mass analyzer (APM) system,[17,28] or the very similar instrument, the centrifugal particle mass analyzer (CPMA).[29] Effective densities can also be studied using other methods, where the mass is not explicitly measured.[19,30−32] The DMA-APM technique has a high precision in the mass measurement and often a high enough resolution to distinguish externally mixed particles, as is typical for urban air. Although suggested as early as 2002, only two complete studies have been published on the mass-mobility relationship or effective density in the ambient air using the technique.[33,34] Limited data sets are also found in McMurry et al.[17] and Park et al.[35] None of the measurements reported have been performed in Europe.

The aim of this study was to investigate the particle effective density, mass-mobility relationship, and mixing state with respect to particle density in an urban environment. Measurements were performed in central Copenhagen during wintertime using a DMA-APM instrument configuration as the main method of investigation. We relate the results to particle origin, morphology, and aging. A year later, complementary measurements using the same methodology were performed at a rural background site located 45 km from the Copenhagen metropolitan area.

EXPERIMENTAL SECTION

Site Description and Measurement Period. The measurements of the urban aerosol were performed at ground level (2 m) in an open street canyon in central Copenhagen, Denmark (55°41′ N, 12°34′ E). The annual daily average of vehicles passing the street in 2012 was 26800, whereof 2.2% were heavy-duty vehicles. A total of 35% of the light-duty vehicles were diesel powered. The measurements were performed during winter (January to February 2012), resulting in a total of 156 h of quality assured DMA-APM data over a period of 38 days.

Measurements at the rural background station (Vavihill, Sweden, 56°01′ N, 13°09′ E[37]) were carried out at the same time of year as those in Copenhagen, but a year later. The station is located about 45 km northeast of Copenhagen. A total of 100 h of data were recorded over a period of 23 days.

More information about the measurement periods and data coverage can be found in the Supporting Information (SI).

Particle Characterization. All instruments were placed indoors. A schematic picture of the experimental setup is given in the SI (Figure S1). The main instruments and methods used are briefly described below. More details and other analysis tools used (scanning mobility particle sizer [SMPS], NO_x monitor, and high resolution transmission electron microscopy [HR-TEM]) are found in the SI. The setup also includes a drier.[36]

DMA-(TD)-APM. In-situ measurements of effective density and the mass-mobility relationship were performed using an aerosol particle mass analyzer (APM, model 3600, Kanomax, Japan) placed downstream from a differential mobility analyzer (DMA, model 3071, TSI Inc., USA). The DMA-APM system measures the mass distribution of individual particles of a certain mobility diameter, d_m. Briefly, the APM consists of two concentric cylinders rotating at the same angular speed. By applying a voltage between the cylinders, charged particles of a specific mass are maintained in the orbit by the electrical force and thus pass the APM. The particles are detected by a CPC (model 7610, TSI Inc., USA) upon exiting the APM. The APM voltage is changed in steps for each setting, resulting in a distribution as a function of voltage.

The acquired voltage distribution spectra were evaluated by fitting one or two normal distribution functions. The spectra were well described by a normal distribution. Simulations performed using the uniform flow model[28] of the DMA-APM transfer function showed that for our DMA-APM settings, a normal distribution captures the distribution peak value. The particle mass was estimated from voltage according to the equations provided in earlier publications.[17,22] The effective density was determined by combining the mobility diameter of the selected particles (set by the DMA) with the mass of the particles derived from the APM according to eq 2. The relative number fractions of the fitted modes were estimated from the fitted intensity parameters, after compensating for the effect of the DMA-APM transfer function that varied with voltage. The APM transfer function broadens the voltage distribution spectra with increasing voltage, while the intensity maxima decreases. As a result, the integral of a measured distribution (propor-

dx.doi.org/10.1021/es5000353 | Environ. Sci. Technol. 2014, 48, 6300−6308

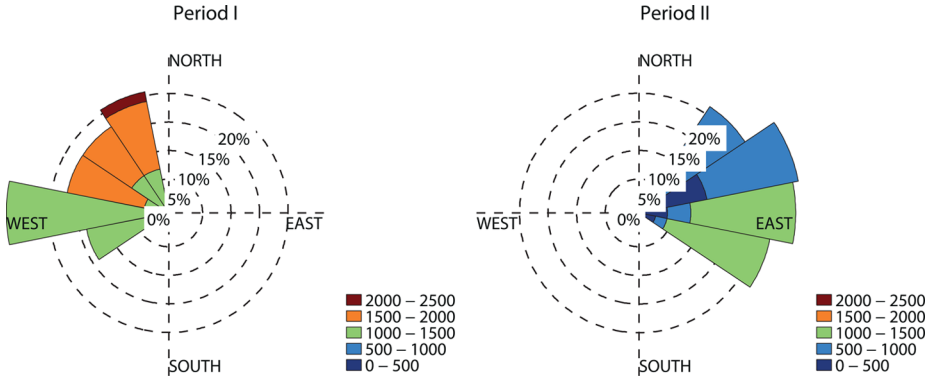

Figure 1. Air mass origin for Periods I and II. The radius of each segment represents the number of trajectories with a center of gravity placed in the direction of the segment; the color represents the distance to the center of gravity in kilometers.

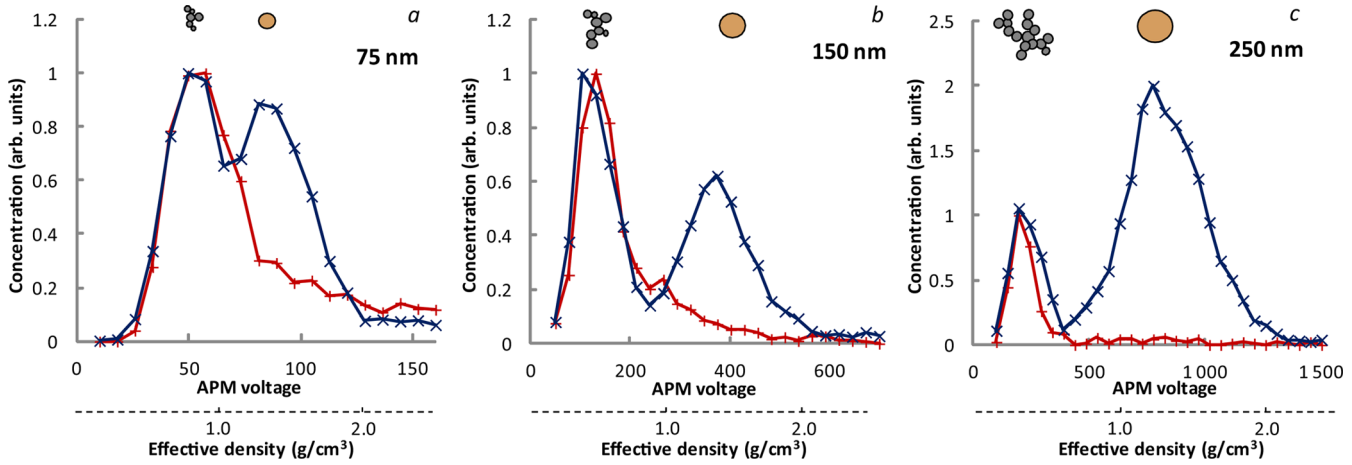

Figure 2. Examples of measured DMA-APM spectra for particles of diameters: (a) 75 nm, (b) 150 nm, and (c) 250 nm. The spectra shown are from 13 Jan. (red curves [+], Period I*a*) and 27 Jan. (blue curves [×], Period II*a*) to illustrate conditions with minor (red) and major (blue) influence of long-range transport. The spectra are normalized with respect to intensity of the soot mode. The corresponding particle effective density is given on the secondary axis (dashed). Note that the spectra are raw APM spectra, not inverted and that the DMA-APM transfer function broadens and decreases the peak of the mass spectra with increasing voltage.[28]

tional to the particle number) varies only weakly with voltage when the mobility size and APM rotational speed is kept constant—as is the case during each DMA-APM scan.

For the urban aerosol, particles of diameters 75, 100, 150, 250, and 350 nm were selected. On a few occasions also sizes of 50, 200, 300, and 400 nm were studied. The results from the latter sizes are not included in Table 1 since the aerosol number fractions are not representative for the entire periods defined. This is because they were not measured continuously and the number fractions are strongly biased by the time of day at which they were measured. The DMA-APM system was calibrated using polystyrene latex spheres (Duke Scientific Corp., USA) of three diameters (100, 240, 350 nm), according to the calibration procedure suggested by McMurry et al. (2002).[17] The principle of the system and more general details are found in Ehara et al.[28] and McMurry et al.[17] More details about the specific DMA-APM used, estimation of errors, etcetera, are found in Rissler et al.[22] The resolution parameter, λ_c, of the DMA-APM settings used was calculated (defined in ref 28) and is given in the SI, Table S2.

An optional thermodenuder (TD), operated at 300 °C, was placed between the DMA and APM, and was used for estimations of the volatile mass fraction of the particles. The particle residence time was ∼10 s. The TD has been evaluated in previous lab studies[36−39] using a similar setup. For more details of the TD, see the study by Malik and coauthors.[38]

The DMA-APM can distinguish between singly and doubly charged particles, if spherical. For aggregates, which have decreasing effective densities with size, this is not always the case. Then the occurrence of doubly charged particles may lead to overestimations of the effective density.[22] The impact of doubly charged particles is often minor, but for measurements of sizes smaller than the peak of the number size distribution, and especially for polydisperse distributions of high mean diameters, the effect needs to be considered. To test the potential errors due to doubly charged particles in this study, the fraction of doubly charged particles was estimated from the number size distributions for each size selected by the DMA-APM system, assuming a Boltzman charge distribution. On average, the doubly charged particles corresponded to 13(±4)% (SD). Assuming that all particles were aggregated (corresponding to the worst case), this would result in an overestimation of mass by less than 5% according to sensitivity tests.[22]

Aerosol Mass Spectrometer (HR-ToF-AMS). The chemical composition of nonrefractory particulate mass (NR-PM) was measured online by means of a high-resolution time-of-flight aerosol mass spectrometer (HR-ToF-AMS, Aerodyne Research Inc., USA).[40] Data analysis was performed with IGOR Pro 6

dx.doi.org/10.1021/es5000353 | *Environ. Sci. Technol.* 2014, 48, 6300−6308

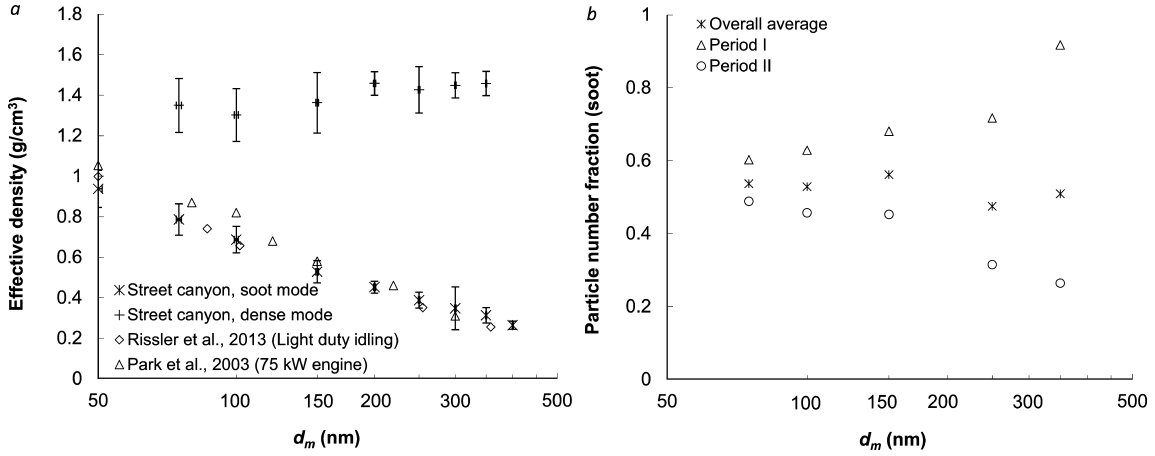

Figure 3. (a) The average effective densities. Error bars correspond to one standard deviation. For comparison, the effective densities of freshly emitted particles from a light duty vehicle during idling[22] and the average of the 75 kW John Deere engine from ref 18, are also plotted. (b) The particle number fraction of the aggregated fresh soot particles during the campaign in Copenhagen.

(Wavemetrics, USA), SQUIRREL 1.51, and PIKA 1.1. The elemental analysis parametrization and fragmentation patterns suggested by Aiken et al.[41] were used.

Wind Trajectories and Selected Periods. The trajectory model Hysplit 4[42] was used to determine the origin of the air masses affecting Copenhagen during the measurement period. The meteorological data required to run the model were obtained from the Global Data Assimilation System (GDAS) by the National Center of Environmental Predictions (NCEP). 72-h back trajectories that arrived at 100 m above ground in Copenhagen were calculated hourly, and a center of gravity was derived for each trajectory. The azimuth angle and distance between center of gravity and the measurement site was then calculated.

During the period when the measurements were performed, two general wind directions prevailed (Figure 1). The wind came either from the west/northwest (Period I) or from the east (Period II). On the basis of the back trajectories, three shorter time periods were also defined: Period I*a*, Period II*a*, and Period II*b*. Period I*a* was very clean with air masses coming from the northwest. During Period II*a* the air mass had traveled over a polluted area southeast of Copenhagen. Period IIb was also a part of Period II, but in this short period the air mass had traveled over a cleaner area than in Period II*a*. More details about the selected periods and the trajectories are provided in the SI.

RESULTS AND DISCUSSION

Particle Effective Densities. The airborne particles found at street level in Copenhagen were externally mixed consisting of (1) porous aggregates of low effective densities, decreasing with increasing size, and (2) dense particles with no typical density trend with size. In this study "externally/internally mixed" refers to the particle effective densities, not necessarily reflecting the chemical composition. The effective density of each group of particles was determined from each distribution as described in the method section. Examples of measured distributions are shown in Figure 2.

The density of each of the two groups of particles was relatively stable over time, whereas the relative contribution of each group varied over time, as illustrated in Figure 2 and discussed in more detail later. The average effective densities and aerosol fractions are presented in Figure 3 and Table 1.

The dense particles had an average effective density (dry) of around 1.4 ± 0.1 g/cm^3 (±1 SD). This leads to the conclusion that these particles were not aggregated, which was confirmed by TEM (Figure 4). The observed densities were similar to those reported previously in the rural and pristine background (1.4 g/cm^3 for Amazonian ambient sampling[43,44] and 1.3 g/cm^3 for organically dominated ambient aerosol[45]) and showed a weak dependence on air mass history, with a trend of lower effective densities during periods with the air mass coming from the west and northwest (Period I).

The effective densities of the porous particles showed the typical features of open aggregates formed by diffusion-limited cluster aggregation (DCLA), with decreasing densities as a function of mobility diameter—in this case ranging from 0.94 g/cm^3 for 50 nm particles down to 0.26 g/cm^3 for 400 nm particles. The mass-mobility relationship and effective density was well described by a power law function with K = 0.022 and ε_m = 2.40 (according to eqs 1 and 2, using SI units: [m] and [kg]). The particle effective densities and power law function describing the mass-mobility relationship of particles found in downtown Copenhagen were very similar to, or in the lower range of, those found for freshly emitted diesel particles generated and characterized under well-controlled lab conditions.[18,20−22]

An analysis of the TEM samples collected at two occasions (analyzing in total 100 primary particles) revealed a primary particle diameter of 29 ± 11 nm (±1 SD). This is in good agreement with the primary particle size of 31 nm estimated from DMA-APM measurements, according to the method suggested by Rissler et al.[22] (K_{forced} = 0.0054, [eq 6[22] note the corrigendum of the constants in the equation]). Analysis by HR-TEM confirmed that the primary particles of the agglomerates had the typical microstructure of soot[22,46] (Figure 4).

There were no observations of particles with effective densities in between the two groups of particles defined, nor were any clear occasional shifts in the effective density observed. This is opposed to the observations made in the two previous studies of atmospheric particles using the DMA-APM.

During the process of atmospheric aging, the effective densities of the soot particles will gradually increase due to the condensation of secondary aerosol mass including secondary

dx.doi.org/10.1021/es5000353 | Environ. Sci. Technol. 2014, 48, 6300−6308

Table 1. Average Densities of the Two Particle Types (Soot Particles, $\rho_{eff,soot}$, and Dense Particles, $\rho_{eff,dense}$) and Relative Aerosol Number Fractions (NF) - Overall Averages and Averaged during the Selected Periods[a]

size (nm)	$\rho_{eff,soot}$	$\rho_{eff,\ dense}$	NF_{soot}	NF_{dense}
50	0.94 ± 0.09	1.65[b] ± 0.09	0.82[b] ± 0.35	0.18[b]
75	0.78 ± 0.09	1.35 ± 0.13	0.54 ± 0.40	0.46
100	0.69 ± 0.07	1.30 ± 0.13	0.53 ± 0.36	0.47
150	0.53 ± 0.05	1.36 ± 0.15	0.56 ± 0.32	0.44
250	0.39 ± 0.04	1.42 ± 0.11	0.47 ± 0.35	0.53
350	0.31 ± 0.04	1.46 ± 0.06	0.51 ± 0.41	0.49
		Period I		
75	0.81 ± 0.08	1.40 ± 0.18	0.60 ± 0.44	0.40
100	0.70 ± 0.08	1.31 ± 0.15	0.63 ± 0.41	0.37
150	0.53 ± 0.05	1.29 ± 0.20	0.68 ± 0.35	0.32
250	0.38 ± 0.03	1.32 ± 0.16	0.72 ± 0.35	0.28
350	0.30 ± 0.03	1.45 ± 0.01	0.92 ± 0.27	0.08
		Period II		
75	0.77 ± 0.08	1.33 ± 0.10	0.49 ± 0.37	0.51
100	0.68 ± 0.06	1.30 ± 0.12	0.46 ± 0.30	0.54
150	0.52 ± 0.06	1.40 ± 0.11	0.45 ± 0.27	0.55
250	0.39 ± 0.05	1.46 ± 0.07	0.31 ± 0.24	0.69
350	0.32 ± 0.04	1.46 ± 0.06	0.26 ± 0.26	0.74
		Period I*a*		
75	0.80 ± 0.06	1.50 ± 0.17	0.56 ± 0.44	0.44
100	0.68 ± 0.08	1.38 ± 0.19	0.57 ± 0.41	0.43
150	0.51 ± 0.03	1.28 ± 0.17	0.71 ± 0.36	0.29
250	0.37 ± 0.02	1.24[c]	0.90 ± 0.23	0.10
350	0.31 ± 0.03		1.00 ± 0.00	0.00
		Period II*a*		
75	0.75 ± 0.09	1.35 ± 0.07	0.25 ± 0.23	0.75
100	0.66 ± 0.06	1.37 ± 0.07	0.27 ± 0.14	0.73
150	0.52 ± 0.05	1.42 ± 0.04	0.29 ± 0.13	0.71
250	0.39 ± 0.07	1.41 ± 0.04	0.16 ± 0.14	0.84
350	0.33 ± 0.05	1.41 ± 0.05	0.11 ± 0.11	0.89
		Period II*b*		
75	0.79 ± 0.03	1.25 ± 0.14	0.91 ± 0.18	0.09
100	0.68 ± 0.04	1.30 ± 0.12	0.78 ± 0.21	0.22
150	0.52 ± 0.03	1.41 ± 0.12	0.69 ± 0.16	0.31
250	0.39 ± 0.02	1.49 ± 0.06	0.55 ± 0.15	0.45
350	0.29 ± 0.01	1.47 ± 0.04	0.54 ± 0.23	0.46

[a]Standard deviations are not given for NF_{dense} since these are identical to those of NF_{soot}. [b]Since the soot particles dominated by number and the two modes were not resolved, the fit of aerosol fraction and density of the compact group of particles is very uncertain. [c]The number is based on only two spectra when the mode was present.

organic aerosol (SOA), ammonium nitrate, and ammonium sulfate. Eventually the aggregates will start to restructure[25,47,48] through the interaction with atmospheric water or other components with sufficiently high surface tension. The restructuring gives rise to a further increase in effective density. For the smallest particles analyzed in our study (≤75 nm), the two groups of particles found were close in density, and thus an increase in effective density of the soot agglomerates due to aging would be difficult to capture. For larger and more porous aggregates, we estimate that a change in effective density would be detectable if ∼10% or larger, and if it is consistent over several scans. Furthermore, the effect of aggregate restructuring is expected to increase with increasing aggregate size due to the more porous structure. When sampling at the street level (∼2 m), the particles to a high degree originate from the nearest road. However, particles emitted elsewhere in the city are also captured, and on occasions when the traffic intensity is very low at the nearest road, soot particles emitted elsewhere are expected to dominate. On the basis of the observations, we conclude that during the time that the freshly emitted soot particles remain in the city, the aging of particles by condensation of SOA, or by restructuring, is not extensive (<10% change in effective density). We estimate the typical residence time of fresh particles of between 20 min and 1.5 h. The lowest estimate is based on emissions in downtown Copenhagen only (a radius of 3 km), an average wind speed of 5 m/s, and assuming that the street canyons are well ventilated. Since the measurements took place during winter, the photochemical activity and thus atmospheric aging were expected to be slow due to the limited amount of sunlight at this geographical location. During the campaign, the average ozone concentration measured in the urban background during the campaign was 28 ppb, and the average relative humidity was 72 ± 9%. Substantial restructuring at elevated RH (but still subsaturated conditions) only occurs after the soot agglomerates have accumulated a sufficient volume or mass fraction of hygroscopic material (on the order of 20−30% or higher).[25] It should be noted that even if the degree of aging is not extensive enough to be captured by the DMA-APM, some atmospheric processing does occur.

Another observation is that the condensation of volatile material onto the soot agglomerates at the tailpipe upon the emission to the atmosphere of Copenhagen is not markedly different from that found in the lab studies.[18,22] Thus, effective densities determined in laboratory studies are of atmospheric relevance.

Degree of External Mixing. Whereas the particle effective densities were stable over time, the relative contribution from each of the two groups of particles varied considerably. The relative number fraction of fresh soot particles (NF_{soot}) was ∼0.5 when averaged over the entire measurement period, with the exception of 50 nm particles that had a higher fraction of soot aggregates (Table 1). Two types of temporal variability in *NF* were observed: a diel pattern and a dependence of air mass origin.

The typical diel variability of the soot number fraction is shown in Figure 5a. This is the average of measurements performed during five nights and consecutive days (details given in the SI). The lowest fraction of soot aggregates were found during nighttime (00:00−04:00). This coincides with low intensity in the Copenhagen traffic[49] and with low NO concentrations (Figure 5b). Thus, the diel temporal variability in the soot fraction is mainly associated with emissions from local traffic.

The relative occurrence of the two groups of particle varied also with air mass origin. For Period II, when the air often traveled over more polluted areas than in Period I, the relative number of dense particles was higher than for Period I (Figure 3b and Table 1). To further explore this dependence with air mass origin, shorter periods with more homogeneous trajectories were selected, shown in the SI (Figure S2). Examples of typical distributions measured during two of the short periods defined are shown in Figure 2. As can be seen, for the time period with air masses arriving from clean ocean areas, the relative contribution of the dense particles (relative to the locally emitted soot aggregates) was nearly negligible, while for the time period with air masses that had traveled over heavily polluted areas, the contribution of dense particles was large.

dx.doi.org/10.1021/es5000353 | Environ. Sci. Technol. 2014, 48, 6300−6308

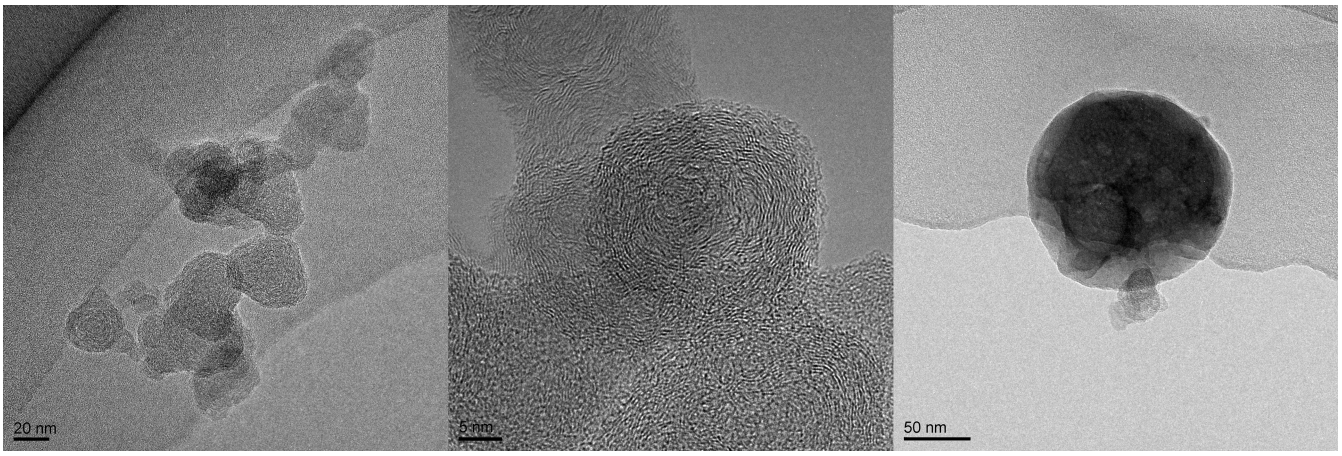

Figure 4. Transmission electron microscope (TEM) images of particles collected in Copenhagen during the measurements. (Left) A TEM image of a typical soot aggregate. (Middle) HR-TEM showing the microstructure of the primary particles of the aggregates. (Right) An image of a typical dense particle.

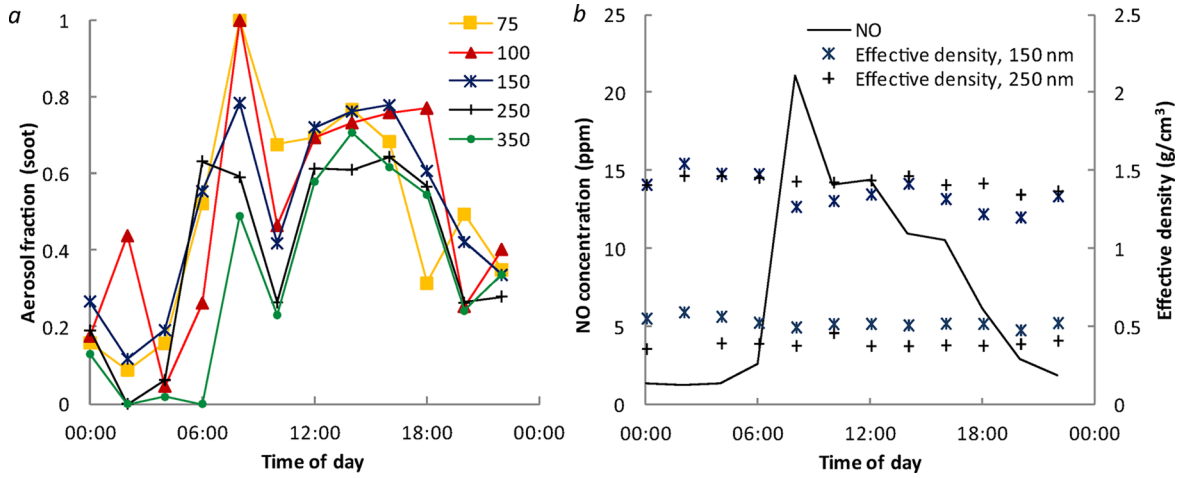

Figure 5. (a) Number fraction of fresh soot aggregates derived from DMA-APM measurements. (b) NO concentrations (used as indicator of traffic) and effective densities of the two groups of particles of sizes 150 and 250 nm (the two series plotted for each size correspond to the two groups of different density).

Thus, the dense particles seem to be a part of a long-range transported background pollution rather than originating from local sources. Similar conclusions were made during a study in a European megacity,[50,51] where the external mixture of the aerosol was studied using a hygroscopicity tandem DMA (H-TDMA). They found particles of an external mixture, with hydrophobic particles resulting from fresh soot emissions, and a background with hygroscopic particles of typical diameter growth factors of 1.6, which is typical for atmospheric salts mixed with some oxidized organics. This is also consistent with the observations and assumptions made by Löndahl et al.[14] based on H-TDMA data.

For Period II the abundance of dense particles tended to increase with increasing size, and vice versa for Period I, as displayed in Figure 3b. From analyzing the particle number size distributions measured in parallel at the rural background site (Vavihill), it became evident that the size dependence of the relative abundance of the two groups of particles was governed by the number size distribution of the long-range transport particles and not by any variability in the size profile of the locally emitted soot particles. The particle number size distributions of the background, continuously monitored at the Vavihill station, are presented in Figure S3, SI. This further strengthens the conclusion that most of the particles with a density of ~1.4 g/cm^3 were from long-range transport.

Effective Densities at the Rural Background Station. To further investigate the effective densities of particles corresponding to the long-range transport observed in Copenhagen, the DMA-APM was brought to the Vavihill rural background site. As expected, in the rural background the dense particles dominated, with an effective density of around 1.4 g/cm^3. This is similar to that of the dense particles observed in Copenhagen. Aggregated particles were only present during occasions with westerly winds. On these occasions, the trajectories did pass nearby Copenhagen, situated approximately 2−3 h upwind, and the aggregates were likely aged soot from the Copenhagen plume. These aggregates had higher effective densities than the soot aggregates found in downtown Copenhagen (~15 to 55% higher), possibly as a result of aging. The effective densities and number fractions found at the rural background site are presented in Table S3.

Volatility. Information about the volatile mass fraction of the particles was gained by introducing a thermodenuder (TD) held at 300 °C in between the DMA and the APM and by

dx.doi.org/10.1021/es5000353 | Environ. Sci. Technol. 2014, 48, 6300−6308

comparing the mass distributions of the selected particles before and after passing the TD. Two typical mass spectra are shown in Figure S4 (SI).

The soot aggregates in the urban environment did not decrease extensively in mass following heating. However, a slight shift in the mass mode was observed, quantified to ∼10%. This would correspond to a 1 nm coating on a 30 nm spherical particle (the soot primary particle size). The soot particle concentrations at the rural background station were too low to allow any determination of the volatile mass fraction.

For the dense particles, the volatile mass fraction was considerably higher. This was the case both in Copenhagen and at the rural background station. The high volatile mass fraction was expected since the major constituents, according to the AMS, were ammonium nitrate, ammonium sulfate, and organic carbon (see next section), all of which volatilize at temperatures below 300 °C. The remaining particle core may be either soot (black carbon), pyrolyzed carbon in the TD, very low volatility organic carbon, or possibly some KCl and K_2SO_4.[51]

From the measurements performed in Copenhagen, it was difficult to quantify the nonvolatile core of the dense particles. This was because it could not be ruled out that part of the mass peak of the nonvolatile core coincided with the mass peak of the nonvolatile soot aggregates. However, from the measurements performed at the rural background site, on occasions when no soot aggregates were present, a rough quantification of the nonvolatile core was made. The core varied from at most ∼20% by mass down to close to zero, varying from day to day, and with a general trend of decreasing core fractions with increasing size.

Chemical Composition. The aerosol mass spectrometer (HR-ToF-AMS) provides information on the chemical composition of the nonrefractory fraction of the particles. The time series of the chemical composition are shown in Figure S5. Diagrams of the average chemical composition, together with the chemical composition of the three shorter periods with homogeneous air mass origin (Periods I*a*, II*a*, and II*b*) are shown in Figure S6. The average particle chemical composition had an organic fraction of 48%, with a carbon mean oxidation state ($\overline{OS}_c$) of −0.8 (as defined by Kroll et al.[52]). This $\overline{OS}_c$ should be compared to that reported for fresh vehicular exhaust particles of −2 and that of heavily aged atmospheric organic aerosol of 0.9.[52,39] Comparing the $\overline{OS}_c$ of the particles present during the three short periods revealed that the period that was most strongly influenced by long-range transport (Period II*a*) also had the most oxidized state (i.e., aged). During that period the $\overline{OS}_c$ were −0.6 compared to −1.2 and −1.0 during the two periods with a lower fraction of dense particles (Period I*a* and Period II*b*, respectively).

The volumetric mass density can be estimated from the chemical composition measured by the HR-ToF-AMS. This is only comparable to the effective density, as focused on in this article, for spherical particles. The soot aggregates are far from spherical, but since the HR-ToF-AMS does not capture the soot, the chemical composition given by the HR-ToF-AMS should closely correspond to that of the dense particles observed with the DMA-APM. For particles >150 nm (these will dominate the PM1 measured by the AMS), the effective density according to the DMA-APM of the dense group of particles was lowest during Period I*a* (∼1.3 g/cm^3). This low density can be explained from the AMS data by the low content of salts such as ammonium nitrate and ammonium sulfate, and relatively high organic content during that period. During the more polluted periods, the inorganic content was higher, resulting in a higher particle density (∼1.4−1.5 g/cm^3). By assuming a density of 1.2 g/cm^3 for the organic fraction, the density according to the DMA-APM could be nearly reproduced when predicted from the chemical composition according to the AMS (1.31, 1.45, and 1.40 g/cm^3 for Period I*a*, Period II*a*, and Period II*b*, respectively).

Further Discussion and Relevance of the Study. Primary soot particles emitted from traffic are often highly aggregated. As soon as the aggregates are emitted to the atmosphere, they will start to undergo transformations. These transformations continues throughout their lifetime, ranging from hours to weeks, slowly filling voids and restructuring the porous aggregates into more dense particles. This results in higher particle effective densities than of the fresh emissions.

The soot transformation time scales are generally not well understood and depend on several parameters such as the availability of precursors for secondary aerosol formation, the UV flux, temperature, and relative humidity. Thus, the time scales of the atmospheric aging may differ considerably from location to location. Pagels and coauthors[25] suggested a characteristic soot transformation time scale to convert aggregates to spheres of 1 to 5 h (1 h for a strongly polluted atmosphere and 5 h for a typical pollution level in the USA) by condensation of sulfuric acid only. Another example of aerosol dynamics and atmospheric chemistry aging time scales can be found in Roldin et al.[53] Here the authors examine how the urban plume from nearby Malmö (∼30 km west of Copenhagen) ages over 24 h during summer clear-sky conditions. Copenhagen in winter represents an environment with low photochemical activity—as is the case for many cities in northern Europe at this time of year.

Copenhagen offered a unique opportunity to study the freshly emitted soot aggregates and the local aging. Emissions of soot from the greater Copenhagen metropolitan area totally dominated over those from surrounding sources, with ship traffic in the waters between Denmark and Sweden, and the Swedish city of Malmö (300 000 inhabitants), as the only significant regional sources. Thus, the aerosol particles analyzed were largely either from long-range transport or emitted locally. The atmospheric relevance of mass-mobility relationships and effective densities of soot generated and characterized under well-controlled laboratory conditions can and have been questioned. However, this study shows that the soot particles in an urban environment may be very similar to those freshly generated in laboratory studies. This has implications for both health effects and climate.

When it comes to the health effects of air pollution, the largest problems associated with exposure to airborne particles are located to urban environments. In this study, we show that about 50% (by number, for particles ≥75 nm) of the submicrometer particles in Copenhagen are aggregated soot particles. This may have important implications when estimating the exposure and respiratory dose. An erroneous assumption of the effective density may lead to an overestimation of the particle mass dose while underestimating the surface area dose,[9,54] when based on measured mobility number size distributions. The results of this study are also of relevance for modeling particle scattering and absorption cross sections, as well as for cloud formation, with implications for climate.

■ ASSOCIATED CONTENT

Supporting Information

More detailed information about the study in general, the setup, and details of the results. Several illustrative figures are provided. This material is available free of charge via the Internet at http://pubs.acs.org.

■ AUTHOR INFORMATION

Corresponding Author

*E-mail: jenny.rissler@design.lth.se. Phone: +46-(0)46-2220534. Mobile: +46-(0)70-1518426. Fax: +46-(0)46-2224709.

Present Addresses

[#]M.F. is currently at DONG Energy, Kraftværksvej 53, DK-7000 Fredericia, Denmark.

[⊥]S.S. is currently at University of Applied Sciences and Arts Northwestern Switzerland, Brugg-Windisch, Switzerland.

Notes

The authors declare no competing financial interest.

■ ACKNOWLEDGMENTS

This research was supported by the Swedish Governmental Agency for Innovation Systems (VINNOVA) through Projects 2009-01117 and 2010-01004, the Swedish Research Council for Environmental, Agricultural Sciences and Spatial Planning (FORMAS) through Projects 216-2009-1294, 2009-615, and 2010-167. Part of this research was also supported by the EU FP7 ACTRIS Project (Aerosols, Clouds, and Trace gases Research Infra Structure Network; EU INFRA-2010-1.1.16-262254), the Swedish Strategic Research Program MERGE (Modeling the Regional and Global Earth System), and the Lund Centre for Studies of Carbon Cycle and Climate Interaction − LUCCI.

■ REFERENCES

(1) Ruckerl, R.; Schneider, A.; Breitner, S.; Cyrys, J.; Peters, A. Health effects of particulate air pollution: A review of epidemiological evidence. *Inhalation Toxicology* **2011**, *23* (10), 555−592.

(2) Brook, R. D.; Rajagopalan, S.; Pope, C. A.; Brook, J. R.; Bhatnagar, A.; Diez-Roux, A. V.; Holguin, F.; Hong, Y. L.; Luepker, R. V.; Mittleman, M. A.; Peters, A.; Siscovick, D.; Smith, S. C.; Whitsel, L.; Kaufman, J. D.; Epidemiol, A. H. A. C.; Dis, C. K. C.; Metab, C. N. P. A. Particulate Matter Air Pollution and Cardiovascular Disease An Update to the Scientific Statement From the American Heart Association. *Circulation* **2010**, *121* (21), 2331−2378.

(3) Bond, T. C.; Doherty, S. J.; Fahey, D. W.; Forster, P. M.; Berntsen, T.; DeAngelo, B. J.; Flanner, M. G.; Ghan, S.; Karcher, B.; Koch, D.; Kinne, S.; Kondo, Y.; Quinn, P. K.; Sarofim, M. C.; Schultz, M. G.; Schulz, M.; Venkataraman, C.; Zhang, H.; Zhang, S.; Bellouin, N.; Guttikunda, S. K.; Hopke, P. K.; Jacobson, M. Z.; Kaiser, J. W.; Klimont, Z.; Lohmann, U.; Schwarz, J. P.; Shindell, D.; Storelvmo, T.; Warren, S. G.; Zender, C. S. Bounding the role of black carbon in the climate system: A scientific assessment. *J. Geophys. Res.- [Atmos.]* **2013**, *118* (11), 5380−5552.

(4) Janssen, N. A.; Gerlofs-Nijland, M. E.; Lanki, T.; Salonen, R. O.; Cassee, F.; Hoek, G.; Fischer, P.; Brunekreef, B.; Krzyzanowski, M., Health effects of black carbon. *Health Effects of Black Carbon*; World Health Organization, Copenhagen, Denmark, 2012.

(5) Benbrahim-Tallaa, L.; Baan, R. A.; Grosse, Y.; Lauby-Secretan, B.; El Ghissassi, F.; Bouvard, V.; Guha, N.; Loomis, D.; Straif, K.; Workin, I. A. R. C. M. Carcinogenicity of diesel-engine and gasoline-engine exhausts and some nitroarenes. *Lancet Oncol.* **2012**, *13* (7), 663−664.

(6) *Review of Evidence on Health Aspects of Air Pollution-REVIHAAP. First Results*; World Health Organization Regional Office for Europe: Bonn, 2013.

(7) Maricq, M. M. Chemical characterization of particulate emissions from diesel engines: A review. *J. Aerosol Sci.* **2007**, *38* (11), 1079−1118.

(8) Burtscher, H. Physical characterization of particulate emissions from diesel engines: a review. *J. Aerosol Sci.* **2005**, *36* (7), 896−932.

(9) Rissler, J.; Swietlicki, E.; Bengtsson, A.; Boman, C.; Pagels, J.; Sandstrom, T.; Blomberg, A.; Londahl, J. Experimental determination of deposition of diesel exhaust particles in the human respiratory tract. *J. Aerosol Sci.* **2012**, *48*, 18−33.

(10) Löndahl, J.; Möller, W.; Pagels, J. H.; Kreyling, W. G.; Swietlicki, E.; Schmid, O. Measurement Techniques for Respiratory Tract Deposition of Airborne Nanoparticles: A Critical Review. *J. Aerosol Med. Pulm. Drug Delivery* **2013**, DOI: 10.1089/jamp.2013.1044.

(11) Hussein, T.; Londahl, J.; Paasonen, P.; Koivisto, A. J.; Petaja, T.; Hameri, K.; Kulmala, M. Modeling regional deposited dose of submicron aerosol particles. *Sci. Total Environ.* **2013**, *458*, 140−149.

(12) Messing, M. E.; Svensson, C. R.; Pagels, J.; Meuller, B. O.; Deppert, K.; Rissler, J. Gas-borne particles with tunable and highly controlled characteristics for nanotoxicology studies. *Nanotoxicology* **2013**, *7* (6), 1052−1063.

(13) Alfoldy, B.; Giechaskiel, B.; Hofmann, W.; Drossinos, Y. Size-distribution dependent lung deposition of diesel exhaust particles. *J. Aerosol Sci.* **2009**, *40* (8), 652−663.

(14) Londahl, J.; Massling, A.; Swietlicki, E.; Brauner, E. V.; Ketzel, M.; Pagels, J.; Loft, S. Experimentally Determined Human Respiratory Tract Deposition of Airborne Particles at a Busy Street. *Environ. Sci. Technol.* **2009**, *43* (13), 4659−4664.

(15) Londahl, J.; Pagels, J.; Boman, C.; Swietlicki, E.; Massling, A.; Rissler, J.; Blomberg, A.; Bohgard, M.; Sandstrom, T. Deposition of biomass combustion aerosol particles in the human respiratory tract. *Inhalation Toxicol.* **2008**, *20* (10), 923−933.

(16) Scheckman, J. H.; McMurry, P. H. Deposition of silica agglomerates in a cast of human lung airways: Enhancement relative to spheres of equal mobility and aerodynamic diameter. *J. Aerosol Sci.* **2011**, *42* (8), 508−516.

(17) McMurry, P. H.; Wang, X.; Park, K.; Ehara, K. The relationship between mass and mobility for atmospheric particles: A new technique for measuring particle density. *Aerosol Sci. Technol.* **2002**, *36* (2), 227−238.

(18) Park, K.; Cao, F.; Kittelson, D. B.; McMurry, P. H. Relationship between particle mass and mobility for diesel exhaust particles. *Environ. Sci. Technol.* **2003**, *37* (3), 577−583.

(19) Maricq, M. M.; Ning, X. The effective density and fractal dimension of soot particles from premixed flames and motor vehicle exhaust. *J. Aerosol Sci.* **2004**, *35* (10), 1251−1274.

(20) Olfert, J. S.; Symonds, J. P. R.; Collings, N. The effective density and fractal dimension of particles emitted from a light-duty diesel vehicle with a diesel oxidation catalyst. *J. Aerosol Sci.* **2007**, *38* (1), 69−82.

(21) Barone, T. L.; Lall, A. A.; Storey, J. M. E.; Mulholland, G. W.; Prikhodko, V. Y.; Frankland, J. H.; Parks, J. E.; Zachariah, M. R. Size-Resolved Density Measurements of Particle Emissions from an Advanced Combustion Diesel Engine: Effect of Aggregate Morphology. *Energy Fuel* **2011**, *25* (5), 1978−1988.

(22) Rissler, J.; Messing, M. E.; Malik, A. I.; Nilsson, P. T.; Nordin, E. Z.; Bohgard, M.; Sanati, M.; Pagels, J. H. Effective Density Characterization of Soot Agglomerates from Various Sources and Comparison to Aggregation Theory. *Aerosol Sci. Technol.* **2013**, *47* (7), 792−805.

(23) Sorensen, C. M. The Mobility of Fractal Aggregates: A Review. *Aerosol Sci. Technol.* **2011**, *45* (7), 765−779.

(24) Weingartner, E.; Burtscher, H.; Baltensperger, U. Hygroscopic properties of carbon and diesel soot particles. *Atmos. Environ.* **1997**, *31* (15), 2311−2327.

(25) Pagels, J.; Khalizov, A. F.; McMurry, P. H.; Zhang, R. Y. Processing of Soot by Controlled Sulphuric Acid and Water CondensationMass and Mobility Relationship. *Aerosol Sci. Technol.* **2009**, *43* (7), 629−640.

(26) Ma, X. F.; Zangmeister, C. D.; Gigault, J.; Mulholland, G. W.; Zachariah, M. R. Soot aggregate restructuring during water processing. *J. Aerosol Sci.* **2013**, *66*, 209−219.
(27) Genberg, J.; van der Gon, H. A. C. D.; Simpson, D.; Swietlicki, E.; Areskoug, H.; Beddows, D.; Ceburnis, D.; Fiebig, M.; Hansson, H. C.; Harrison, R. M.; Jennings, S. G.; Saarikoski, S.; Spindler, G.; Visschedijk, A. J. H.; Wiedensohler, A.; Yttri, K. E.; Bergstrom, R. Light-absorbing carbon in Europe - measurement and modelling, with a focus on residential wood combustion emissions. *Atmos. Chem. Phys.* **2013**, *13* (17), 8719−8738.
(28) Ehara, K.; Hagwood, C.; Coakley, K. J. Novel method to classify aerosol particles according to their mass-to-charge ratio - Aerosol particle mass analyser. *J. Aerosol Sci.* **1996**, *27* (2), 217−234.
(29) Olfert, J. S.; Collings, N. New method for particle mass classification - the Couette centrifugal particle mass analyzer. *J. Aerosol Sci.* **2005**, *36* (11), 1338−1352.
(30) Pitz, M.; Cyrys, J.; Karg, E.; Wiedensohler, A.; Wichmann, H. E.; Heinrich, J. Variability of apparent particle density of an urban aerosol. *Environ. Sci. Technol.* **2003**, *37* (19), 4336−4342.
(31) Kannosto, J.; Virtanen, A.; Lemmetty, M.; Makela, J. M.; Keskinen, J.; Junninen, H.; Hussein, T.; Aalto, P.; Kulmala, M. Mode resolved density of atmospheric aerosol particles. *Atmos Chem. Phys.* **2008**, *8* (17), 5327−5337.
(32) Slowik, J. G.; Stainken, K.; Davidovits, P.; Williams, L. R.; Jayne, J. T.; Kolb, C. E.; Worsnop, D. R.; Rudich, Y.; DeCarlo, P. F.; Jimenez, J. L. Particle morphology and density characterization by combined mobility and aerodynamic diameter measurements. Part 2: Application to combustion-generated soot aerosols as a function of fuel equivalence ratio. *Aerosol Sci. Technol.* **2004**, *38* (12), 1206−1222.
(33) Geller, M.; Biswas, S.; Sioutas, C. Determination of particle effective density in urban environments with a differential mobility analyzer and aerosol particle mass analyzer. *Aerosol Sci. Technol.* **2006**, *40* (9), 709−723.
(34) Levy, M. E.; Zhang, R.; Khalizov, A. F.; Zheng, J.; Collins, D. R.; Glen, C. R.; Wang, Y.; Yu, X. Y.; Luke, W.; Jayne, J. T. Measurements of submicron aerosols in Houston, Texas during the 2009 SHARP field campaign. *J. Geophys. Res., [Atmos.]* **2013**, *118* (18), 10518−10534.
(35) Park, K.; Dutcher, D.; Emery, M.; Pagels, J.; Sakurai, H.; Scheckman, J.; Qian, S.; Stolzenburg, M. R.; Wang, X.; Yang, J.; McMurry, P. H. Tandem measurements of aerosol properties - A review of mobility techniques with extensions. *Aerosol Sci. Technol.* **2008**, *42* (10), 801−816.
(36) Sjogren, S.; Frank, G. P.; Berghof, M. I. A.; Martinsson, B. G. Continuous stand-alone controllable aerosol/cloud droplet dryer for atmospheric sampling. *Atmos. Meas. Tech.* **2013**, *6* (2), 349−357.
(37) Tunved, P.; Hansson, H. C.; Kulmala, M.; Aalto, P.; Viisanen, Y.; Karlsson, H.; Kristensson, A.; Swietlicki, E.; Dal Maso, M.; Strom, J.; Komppula, M. One year boundary layer aerosol size distribution data from five nordic background stations. *Atmos. Chem. Phys.* **2003**, *3*, 2183−2205.
(38) Malik, A.; Nilsson, P. T.; Pagels, J.; Lindskog, M.; Rissler, J.; Gudmundsson, A.; Bohgard, M.; Sanati, M. Methodology for Sampling and Characterizing Internally Mixed Soot-Tar Particles Suspended in the Product Gas from Biomass Gasification Processes. *Energy Fuel* **2011**, *25* (4), 1751−1758.
(39) Wittbom, C.; Pagels, J. H.; Rissler, J.; Eriksson, A. C.; Carlsson, J. E.; Roldin, P.; Nordin, E. Z.; Nilsson, P. T.; Swietlicki, E.; Svenningsson, B. Cloud droplet activity changes of soot aerosol upon smog chamber ageing. *Atmos. Chem. Phys. Discuss.* **2014**, *14*, 8851−8914.
(40) DeCarlo, P. F.; Kimmel, J. R.; Trimborn, A.; Northway, M. J.; Jayne, J. T.; Aiken, A. C.; Gonin, M.; Fuhrer, K.; Horvath, T.; Docherty, K. S.; Worsnop, D. R.; Jimenez, J. L. Field-deployable, high-resolution, time-of-flight aerosol mass spectrometer. *Anal. Chem.* **2006**, *78* (24), 8281−8289.
(41) Aiken, A. C.; Decarlo, P. F.; Kroll, J. H.; Worsnop, D. R.; Huffman, J. A.; Docherty, K. S.; Ulbrich, I. M.; Mohr, C.; Kimmel, J. R.; Sueper, D.; Sun, Y.; Zhang, Q.; Trimborn, A.; Northway, M.; Ziemann, P. J.; Canagaratna, M. R.; Onasch, T. B.; Alfarra, M. R.; Prevot, A. S. H.; Dommen, J.; Duplissy, J.; Metzger, A.; Baltensperger, U.; Jimenez, J. L. O/C and OM/OC ratios of primary, secondary, and ambient organic aerosols with high-resolution time-of-flight aerosol mass spectrometry. *Environ. Sci. Technol.* **2008**, *42* (12), 4478−4485.
(42) Draxler, R. R.; Hess, G. Description of the HYSPLIT4 modeling system. 1997.
(43) Rissler, J.; Vestin, A.; Swietlicki, E.; Fisch, G.; Zhou, J.; Artaxo, P.; Andreae, M. O. Size distribution and hygroscopic properties of aerosol particles from dry-season biomass burning in Amazonia. *Atmos. Chem. Phys.* **2006**, *6*, 471−491.
(44) Chen, Q.; Farmer, D. K.; Schneider, J.; Zorn, S. R.; Heald, C. L.; Karl, T. G.; Guenther, A.; Allan, J. D.; Robinson, N.; Coe, H.; Kimmel, J. R.; Pauliquevis, T.; Borrmann, S.; Poschl, U.; Andreae, M. O.; Artaxo, P.; Jimenez, J. L.; Martin, S. T., Mass spectral characterization of submicron biogenic organic particles in the Amazon Basin. *Geophys. Res. Lett.* **2009**, *36*.
(45) Cross, E. S.; Slowik, J. G.; Davidovits, P.; Allan, J. D.; Worsnop, D. R.; Jayne, J. T.; Lewis, D. K.; Canagaratna, M.; Onasch, T. B. Laboratory and ambient particle density determinations using light scattering in conjunction with aerosol mass spectrometry. *Aerosol. Sci. Technol.* **2007**, *41* (4), 343−359.
(46) Happonen, M.; Lahde, T.; Messing, M. E.; Sarjovaara, T.; Larmi, M.; Wallenberg, L. R.; Virtanen, A.; Keskinen, J. The comparison of particle oxidation and surface structure of diesel soot particles between fossil fuel and novel renewable diesel fuel. *Fuel* **2010**, *89* (12), 4008−4013.
(47) Khalizov, A. F.; Lin, Y.; Qiu, C.; Guo, S.; Collins, D.; Zhang, R. Y. Role of OH-Initiated Oxidation of Isoprene in Aging of Combustion Soot. *Environ. Sci. Technol.* **2013**, *47* (5), 2254−2263.
(48) Cappa, C. D.; Onasch, T. B.; Massoli, P.; Worsnop, D. R.; Bates, T. S.; Cross, E. S.; Davidovits, P.; Hakala, J.; Hayden, K. L.; Jobson, B. T.; Kolesar, K. R.; Lack, D. A.; Lerner, B. M.; Li, S. M.; Mellon, D.; Nuaaman, I.; Olfert, J. S.; Petaja, T.; Quinn, P. K.; Song, C.; Subramanian, R.; Williams, E. J.; Zaveri, R. A. Radiative Absorption Enhancements Due to the Mixing State of Atmospheric Black Carbon. *Science* **2012**, *337* (6098), 1078−1081.
(49) Ketzel, M.; Wahlin, P.; Berkowicz, R.; Palmgren, F. Particle and trace gas emission factors under urban driving conditions in Copenhagen based on street and roof-level observations. *Atmos. Environ.* **2003**, *37* (20), 2735−2749.
(50) Juranyi, Z.; Tritscher, T.; Gysel, M.; Laborde, M.; Gomes, L.; Roberts, G.; Baltensperger, U.; Weingartner, E. Hygroscopic mixing state of urban aerosol derived from size-resolved cloud condensation nuclei measurements during the MEGAPOLI campaign in Paris. *Atmos Chem. Phys.* **2013**, *13* (13), 6431−6446.
(51) Laborde, M.; Crippa, M.; Tritscher, T.; Juranyi, Z.; Decarlo, P. F.; Temime-Roussel, B.; Marchand, N.; Eckhardt, S.; Stohl, A.; Baltensperger, U.; Prevot, A. S. H.; Weingartner, E.; Gysel, M. Black carbon physical properties and mixing state in the European megacity Paris. *Atmo.s Chem. Phys.* **2013**, *13* (11), 5831−5856.
(52) Kroll, J. H.; Donahue, N. M.; Jimenez, J. L.; Kessler, S. H.; Canagaratna, M. R.; Wilson, K. R.; Altieri, K. E.; Mazzoleni, L. R.; Wozniak, A. S.; Bluhm, H.; Mysak, E. R.; Smith, J. D.; Kolb, C. E.; Worsnop, D. R. Carbon oxidation state as a metric for describing the chemistry of atmospheric organic aerosol. *Nat. Chem.* **2011**, *3* (2), 133−139.
(53) Roldin, P.; Swietlicki, E.; Massling, A.; Kristensson, A.; Londahl, J. L.; Eriksson, A.; Pagels, J.; Gustafsson, S. Aerosol ageing in an urban plume - implication for climate. *Atmos Chem. Phys.* **2011**, *11* (12), 5897−5915.
(54) Eggersdorfer, M. L.; Grohn, A. J.; Sorensen, C. M.; McMurry, P. H.; Pratsinis, S. E. Mass-mobility characterization of flame-made ZrO_2 aerosols: Primary particle diameter and extent of aggregation. *J. Colloid Interface Sci.* **2012**, *387*, 12−23.